11 Infection and Inflammation Imaging

Ora Israel, Enrique Estrada-Lobato, and Thomas Neil Pascual

11.1 Clinical Indications

Commonly evaluated pediatric infectious processes [1–3]:

- Musculoskeletal (MSK) infections
  - Osteomyelitis (diagnosis, differential diagnosis, single vs. multifocal disease)
  - Discitis
  - Arthritis
- Fever of unknown origin (FUO) is at present evaluated with FDG imaging as a second-line diagnostic investigations. The test has high overall performance, mainly in:
  - Immune-compromised children [4–6].
  - Febrile neutropenia (absolute neutrophil count below 500/mm^3) in immune-suppressed and/or cancer patients [7].

Additional indications in children [8]

- Fungal infections (e.g., aspergillosis and candidiasis).
- Inflammatory bowel disease (IBD) (diagnosis, extent of disease, differential diagnosis of active disease vs. fibrosis, treatment evaluation) [9].
- Inflammatory processes
  - Vasculitis
  - Chronic granulomatous diseases (e.g., sarcoidosis)

11.2 Pre-exam Information

- Relevant clinical data:
  - Measure and record the patient height and weight.
  - Current symptoms, pertinent physical findings, duration of signs and symptoms.
  - Pre-existing conditions.
  - Previously or currently received therapy such as antibiotics, corticosteroids, chemotherapy, radiation therapy, and diphosphonates.
  - Prior orthopedic or non-orthopedic surgery, presence of orthopedic hardware.
- Relevant recent imaging studies.

O. Israel (✉)
B&R Rappaport Faculty of Medicine, Technion, Haifa, Israel

E. Estrada-Lobato
Nuclear Medicine and Diagnostic Imaging Section, Division of Human Health, Department of Nuclear Sciences and Applications, International Atomic Energy Agency, Vienna, Austria

T. N. Pascual
Department of Science and Technology, Manila, Philippines

Z. Bar-Sever et al. (eds.), *A Practical Guide for Pediatric Nuclear Medicine*,
https://doi.org/10.1007/978-3-662-67631-8_11

For the activity of all radiotracers to be administered:

Refer to the EANM pediatric dosage card and to the North American consensus guidelines on radiopharmaceutical administration in children in the respective EANM and SNMMI and image gently web sites.

Reference to national regulation guidelines, if available, should be considered.

Study Protocol for Bone Scintigraphy [2, 10]

Patient preparation:

- Good hydration, patients are instructed to drink at least 2 cups after radiotracer injection, before returning for delayed imaging.
- Infants should be fed prior or immediately after injection.
- Children should be encouraged to urinate frequently to reduce the exposure of the bladder.

Radiopharmaceutical, activity, mode of delivery

Radiopharmaceuticals:

- [^{99m}Tc]-MDP (MDP)

Activity:

- 9.3 MBq/kg (0.25 mCi/Kg), minimum dose 40 MBq (1.1 mCi).

Acquisition protocol (Figs. 11.1, 11.2, and 11.3)

- Position: Supine, with the child comfortably secured to the bed, including feet secured with an inward tilt (allows adequate visualization of the fibulae).
- Collimators: High or ultra-high low-energy collimator. Pinhole collimator, if available, can improve detection of lesions in the hip joint.
- Blood flow images: 2–5 s/frame for a total of 60 s, matrix 128 × 128, size appropriate zoom.
- Early blood pool images: torso 300 Kcounts, extremities 150–200 Kcounts.
- Late skeletal phase images are typically acquired 3 h after injection.
- Whole body sweeps: with bed speed adjusted to the child's age [11].
  - 8 cm/min for children aged 4–8 years.
  - 10 cm/min for ages 8–12 years
  - 12 cm/min for ages 12–16 years
  - 15 cm/min over 16 years of age.
  - Multiple spot views (alternatively) to cover the entire skeleton in anterior and posterior projections: matrix 256 × 256, counts: torso 500 Kcounts, skull 300 Kcounts, knees 100–200 Kcounts, hands and feet 50–100 Kcounts. 2nd variant: the time to obtain 500 Kcounts for the torso should be recorded and used to time the acquisition of the other body parts.
- SPECT: 15–30 s/frame, 120 projections, matrix 128 × 128.
- SPECT/CT (when clinically indicated, if available):
  - CT component using pediatric settings with dose modulation.
  - CT field of view to the finding on SPECT, tube setting depending on whether the CT is intended to be acquired as low dose or fully diagnostic CT (range: between 80 and 110 kVp); CT slice thickness 2–2.5 mm with overlapping cuts.

11.3 Study Interpretation of Bone Scintigraphy [12]

- Osteomyelitis is based on increased local blood flow and bone turnover. The scintigraphic pattern is characterized by increased blood flow and blood pool (tissue hyperemia) and focal increased uptake in the skeletal phase (Fig. 11.1).

- Osteomyelitis involves mainly the metaphyseal portion of long bones or the metaphyseal equivalents of irregular bones.
- Less commonly, osteomyelitis presents as diffuse uptake along a segment of a long bone (probably due to periosteal irritation).
- Mandatory whole-body imaging allows the detection of at times unsuspected multifocal disease including sites related to referred pain. Multifocal osteomyelitis is more common in young infants.
- Bone scans can differentiate osteomyelitis from soft tissue infections.
  - Cellulitis presents with diffuse increased blood flow and blood pool in soft tissue adjacent to bony structures and mild diffuse increased tracer activity in the same area on the skeletal phase.
  - Arthritis presents with diffuse uptake in all bony structures of a joint, with or without accompanying findings in the blood flow and blood pool phases.
  - Discitis typically presents as increased uptake in two adjacent vertebral bodies above and below the inflamed disc.
- In most cases, an abnormal bone scan can be seen as early as 24 h from the onset of symptoms.
- Cases with long-standing osteomyelitis show increased blood pool activity surrounding photopenic defects (Fig. 11.2). On the delayed images, there are corresponding cold lesions in keeping with bony abscesses. The differential diagnosis includes infarcted bone.
- Antibiotic therapy does not affect bone scan findings of osteomyelitis in the short run.

Study Protocol for Tc-WBC Scan [8, 13]

Patient preparation:

- Patients do not need to fast and may take all their usual medications.
- The patient should be well hydrated.
- Explain to patients and parents/caregivers that the procedure is long and requires withdrawal of relatively large amounts of blood (considering the specific pediatric population).

Radiopharmaceutical, activity, mode of delivery

Radiopharmaceutical

- [^{99m}Tc]-WBC

Activity

- 3.7–7.4 MBq/kg (0.1–0.2 mCi/Kg), minimum dose 40 MBq (1.1 mCi)

  For detailed instructions regarding the WBC labelling technique, see appropriate guidelines. The blood volume required for WBC labelling has to be adjusted and reduced as much as possible in young infants [14].

Acquisition protocol (Fig 11.4)

- Collimator: low energy, high resolution, parallel hole.
- Scanning field: related to clinical indication should be either whole body or limited FOV to area of clinical complaints.
- Acquisition protocol:
  - Early images, 30 min post-injection, including of the chest and upper abdomen as well as images for in vivo quality control of WBC labelling.
  - Delayed images: 3–4 h post-injection.
  - Late images: 20–24 h post-injection.
- Acquisition parameters—static images:
  - Size appropriate zoom, matrix 256 × 256.
  - Acquisition options:

    Time corrected for isotope decay: early images are acquired with a set number of counts or time, followed by delayed and late images corrected for the 99mTc 6-h half-life. Different images can be com-

pared with the same intensity scale avoiding operator-dependent changes in the image display.
Fixed time/image: 5–10 min/projection. Difficult to interpret because of interfering data from other organs.

- SPECT or SPECT/CT (recommended if available): Usually performed after the delayed step (3–4 h post-injection).
  - SPECT parameters if performed after delayed step: 20–30 sec/step (depending on the injected activity).
  - SPECT can be also added to the late step (20–24 h post-injection) with following parameters:
    30–50 sec/step (depending on the injected activity and FOV to be imaged, longer for peripheral parts, shorter for abdomen).
    Indicated if there are new sites of pathological uptake not seen on earlier scans.
- Modified parameters for IBD: Images acquisition at 30 min and 2–3 h post-injection only (Fig. 11.5).

11.4 Study Interpretation of Tc-WBC Scan [13]

Diagnosis of infection is made by comparing delayed and late images:

- Negative: no uptake or clear decrease of intensity of uptake between delayed and late images.
- Positive: clear increase in intensity and/or size of uptake over time in lesion (Fig 11.4).
- Equivocal, cases such as:
  - Similar/slightly decreasing uptake over time.
  - Slight increase in size and/or intensity over time.

Physiologic biodistribution, pitfalls, and positivity criteria:

- WBCs show a transitory migration to the lungs, followed by accumulation in the spleen and less in the liver and bone marrow.
- Lung uptake early post-injection is physiologic, but at 4 and 24 h, it is abnormal.
- Normal bowel activity is seen in 20–30% of children at 1 h due to *Tc*-HMPAO excretion from the liver.
- Tc-WBCs migrate from spleen and bone marrow to infected tissues. Therefore, in cases with infection there is an increase in uptake over time in sites of disease while bone marrow and spleen activity decrease.
- The rate of Tc-WBC accumulation in infection depends on:
  - Location: earlier in cardio-vascular vs. bone and CNS infection.
  - Virulence: higher in active vs. chronic processes.
  - Pathogen: lower in fungal vs. bacterial infection.
  - Antibiotic or steroid therapy may decrease Tc-WBC uptake.

Study Protocol for [18F] -FDG [2, 6, 15, 16]

Patient preparation:

- Fast: 4 h before tracer injection and during the uptake phase is recommended in adults and adolescents. This duration should be shortened according to age in young children, toddlers, and infants.
- Good hydration with plain, unflavored water.
- Serum glucose level must be measured before radiotracer administration and should be below 200 mg/dL (11.1 mmol/L), preferably below 140 mg/dL (7.8 mmol/L) [17].

Radiopharmaceutical, activity, mode of delivery

Radiopharmaceuticals:

- [^{18}F] -FDG (FDG)

Activity

- 3.7–5.2 MBq/kg (0.1–0.14 mCi/kg) minimum 26 MBq (0.7 mCi).

Acquisition protocol

- Uptake time: 45–60 min.
- Scanning field: related to clinical indication should be either vertex-to-feet or limited FOV to area of clinical complaints.
- Acquisition protocol: 2–4 min/bed position - these parameters will potentially change with the implementation of new PET technology (see also Chap. 10).

11.5 Study Interpretation of FDG

- Positivity criteria: focal or non-focal abnormal tracer uptake.
- False negatives: Lesion located adjacent to and masked by physiologic tracer activity.

11.6 Correlative Imaging [18]

- Plain radiographs are readily available and are associated with a low radiation burden. They are used in children with suspected pulmonary and MSK infections. In patients with a skeletal pathology, this test is used mainly for excluding fractures and bone tumors in the differential diagnosis of suspected osteomyelitis.
- US is primarily used to investigate soft tissue infections and inflammatory processes.
- CT is readily available at present. Radiation exposure can be reduced by employing specialized pediatric protocols. As a component of SPECT/CT and PET/CT, it can increase the specificity and accuracy of nuclear medicine tests.
- MRI advantages stem from its lack of ionizing radiation. It also has higher soft tissue contrast than CT.

11.7 Red Flags [2]

Tc-MDP

- Cannot distinguish between infectious and non-infectious arthritis.
- Cannot differentiate between infection and malignancies, such as osteosarcoma.
- Cannot detect extension of spinal infection from the disc to the adjacent soft tissues. These findings are best evaluated with MRI.
- In cases of discitis, there may be a lag of one week between the onset of symptoms and the first appearance on the bone scan.
- A negative bone scan in the presence of persistent fever does not exclude the diagnosis of arthritis and may reflect pyomyositis and needs to be further assessed.

WBC

- Children with severe neutropenia may lack sufficient leukocytes for adequate WBC labelling.
- The large quantity of blood needed for the procedure is limiting its use in neonates and young children.
- The study has lower performance indices in chronic infections and acute spinal infections.
- Visualization of liver and bowel on later images can produce false positive images in patients with suspected IBD.

FDG

- Radiotracer uptake is not specific to infection.
- Cannot differentiate between infection and (sterile) inflammation.
- Cannot differentiate between infection and malignancy.

Matching of Radiotracers Used for Specific Pediatric Infectious and Inflammatory Processes

- MSK infections
  - Osteomyelitis: Tc-MDP, WBC, FDG
  - Discitis: Tc-MDP, FDG
  - Arthritis: Tc-MDP, FDG
- FUO (including febrile neutropenia): FDG (Figs. 11.6, 11.7, 11.8 and 11.9)
- IBD: FDG, WBC
- Fungal infections: FDG
- Inflammatory processes
  - Vasculitis: FDG (Fig. 11.10)
  - Chronic granulomatous diseases: FDG

11.8 Take Home Messages

- Knowledge regarding the pre-test probability of infection is essential:
  - In low pre-test probability of infection and suspected chronic or non-bacterial processes, FDG imaging is preferred.
  - In case of high WBC counts, ESR or CRP values: Tc-WBC scan can be the first test.
  - WBC accumulation is generally more specific for infection than increased FDG uptake.
- *For WBC studies:*
  - Images from different time points have to be displayed at the same intensity scale (Figs. 11.4 and 11.5).
  - Any adjustment of the image intensity scale must be applied to all images together to avoid operator bias.
  - Patients receiving antibiotic treatment should not be excluded from performing Tc-WBC scans.
- *For FDG imaging:*
  - Hyperglycemia and antibiotic treatment most probably do not affect significantly the diagnostic potential of the study in suspected infection [19, 20].
  - A specific dietary regimen has to be applied in patients evaluated for the suspicion or monitoring of a cardiac infectious process.

MSK infection [21]:

- Three-phase bone scintigraphy, highly sensitive for diagnosing osteomyelitis in uncomplicated bones is suboptimal in patients with pre-existing fracture or orthopedic hardware. Bone scintigraphy in non-oncological indications is further discussed in detail in Chap. 10.
- Hybrid imaging is associated with a significant improvement in specificity (Figs. 11.3 and 11.6). The SPECT/PET component detects the presence of an active process while on the CT component characteristic findings include areas of cortical destruction and adjacent soft tissue abscess or empyema.
- Labelled WBC has been reported in only limited studies/cases of MSK infection in children. If at all, in cases of MSK pathologies this test usually follows bone scintigraphy.
- FDG imaging shows high-performance indices even in challenging settings such as [22]:
- Chronic and/or low-grade MSK infection (Fig 11.6).
  - In the axial skeleton, including cases with suspected spinal fusion hardware infection (superior to WBC).
  - FDG imaging can also detects extraosseous lesions.

FUO [6, 16, 23, 24]

- In children with FUO, the performance indices are similar to those reported in adults.
- Has a higher positive yield in children with fever early during the disease (less than 3 months), and in those with abnormal laboratory investigations (leukocytosis, neutrophilia, high CRP, ESR) (Figs. 11.6, 11.7, 11.8, and 11.9).
- Can identify organs or tissues likely to contain the source of fever, thus guiding further tests including tissue sampling procedures.
- Has a high NPV and it is thus unlikely to find a focal etiology of FUO in cases with a negative study.

11.9 Representative Case Examples

Case 11.1 Osteomyelitis, Tc-MDP (Fig. 11.1)

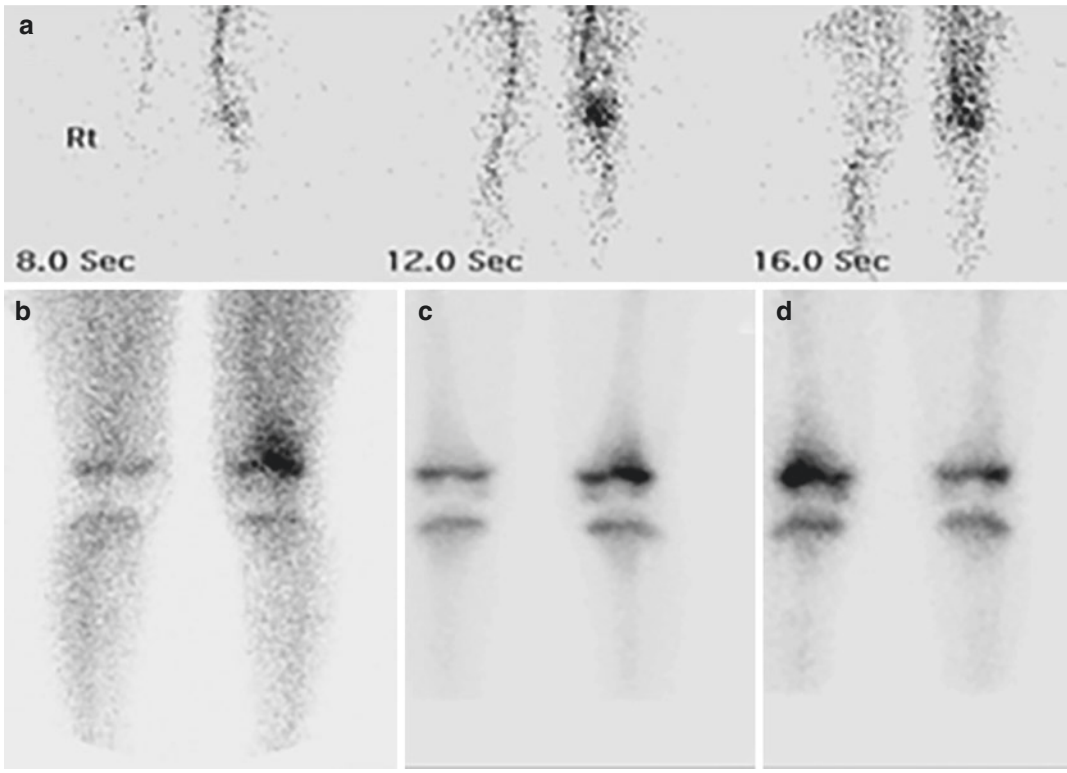

Fig. 11.1 History: A 6-year-old boy presented with a painful left knee. Radiographs were normal, and blood CRP and ESR were elevated. A whole-body bone scan was performed after injection of Tc-MDP. Study report: The dynamic (**a**) and blood pool (**b**) images show increased perfusion and hyperemia to the upper part of the left knee. Delayed planar scintigraphy of the region of the knees (anterior view, **c**, and posterior view, **d**) shows focal increased tracer uptake in the left distal femoral metaphysis. The remainder of the whole-body scan was normal (not shown). Impression: The findings are suggestive of acute osteomyelitis. Blood cultures grew *Staphylococcus aureus*

Case 11.2 Osteomyelitis, Tc-MDP (Fig. 11.2)

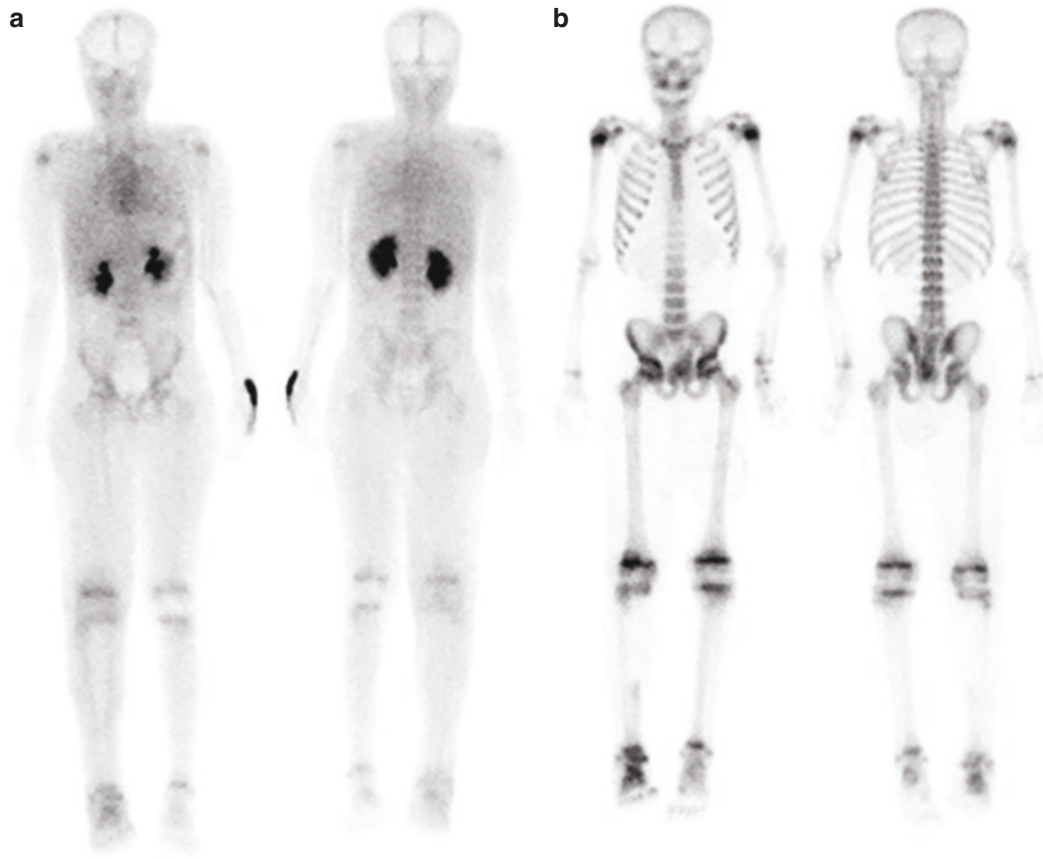

Fig. 11.2 History: A 10-year-old boy had surgery for septic arthritis of the right knee and ankle, with no significant clinical improvement. Bone scintigraphy was performed after injection of Tc-MDP for the suspicion of additional sites of infection. Study report: Early whole-body blood pool scintigraphy, anterior view (**a**, right) shows a rim of increased hyperemia surrounding an area of decreased activity in the right tibia. Increased blood pool activity is also seen in the region of the right knee and foot. Delayed whole-body scintigraphy (**b**) shows a "cold" area of absent radiotracer uptake in the proximal two-thirds of the right tibia and decreased activity in the proximal tibial growth plate. There is also increased tracer uptake in the right knee joint and foot. Impression: The findings of a "cold bone" in this setting suggest a bony abscess or bone necrosis. The child had surgery and a large volume of pus was drained from the tibia, confirming the diagnosis of osteomyelitis

Case 11.3 Osteomyelitis in Complicated Bone, Tc-MDP (Fig. 11.3)

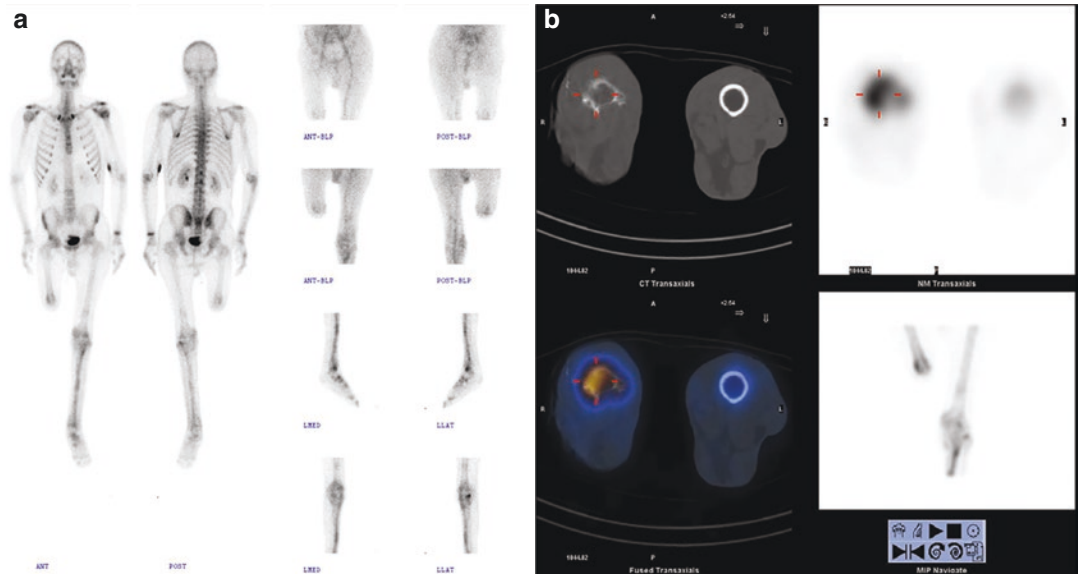

Fig. 11.3 History: An 18-year-old boy with post-traumatic right femoral amputation 18 months prior to this examination presented with a draining fistula from the right femoral stump. Osteomyelitis was suspected and a bone scan was performed after administration of Tc-MDP. Study report: Blood pool images (**a**, upper right quadrant) demonstrate hyperemia at the margin of the right femoral stump. On delayed planar bone scintigraphy (**a** left) there is focal increased tracer activity in the right femoral stump. There is also diffuse increased uptake along the bones of the left calf and foot due to limping. SPECT/CT (**b**) indicates that the area of focal radiotracer uptake in the right femoral stump corresponds to signs of chronic osteomyelitis on the CT component. Impression: The findings suggest chronic osteomyelitis at the right femoral stump

Case 11.4 Infected Hematoma of the Skull, Tc-WBC (Fig. 11.4)

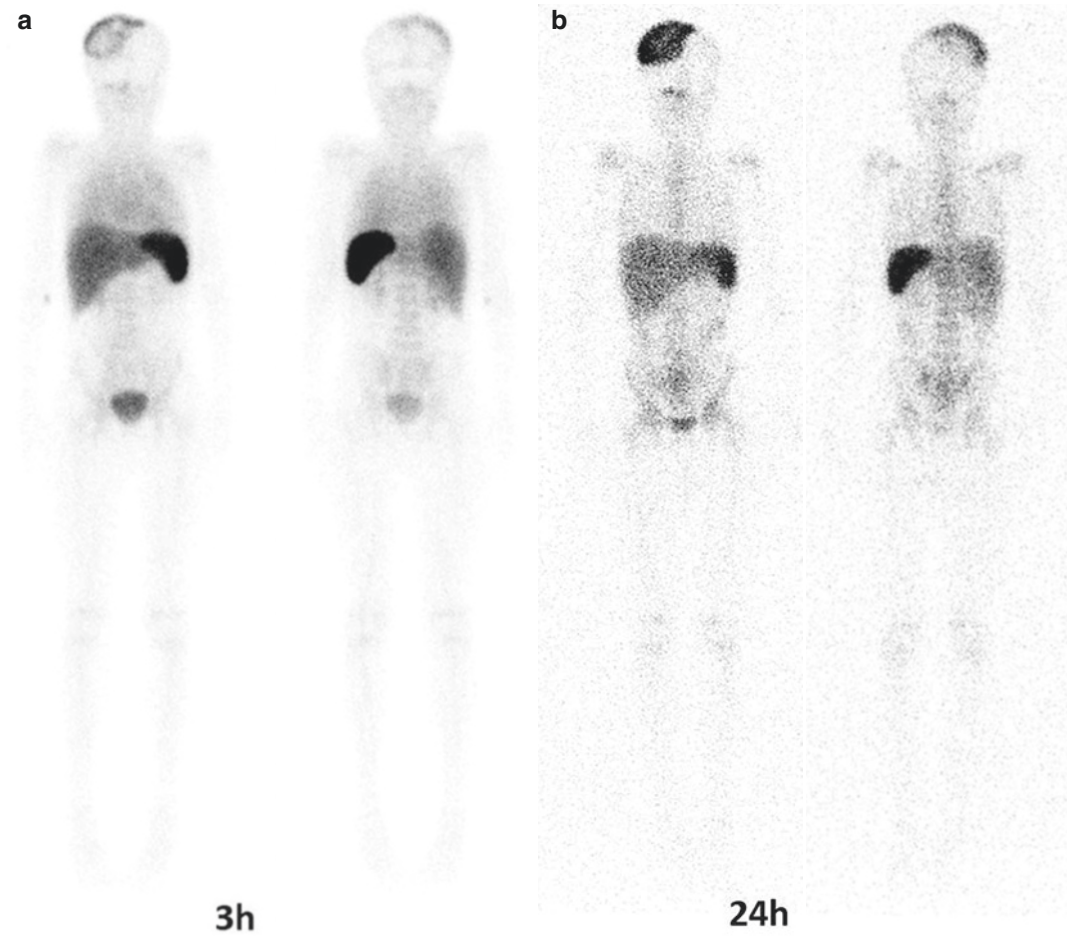

Fig. 11.4 History: A 9-year-old girl presented one day after falling and hitting the right side of her head. She subsequently developed a hematoma and periorbital swelling. She had a 1-year background history of weight loss and proptosis compatible with thyrotoxicosis and developed a thyroid storm after the initial contrast brain CT. Due to ongoing temperature spikes, a blood culture was performed and was positive for *Streptococcus constellatus*, a bacteria known to cause abscess formation. The patient did not respond to appropriate treatment and a Tc-WBC was requested. Study report: On the 3-h whole-body scan (**a**) there is an abnormal accumulation of Tc-WBC in the right-sided skull hematoma, increasing in intensity on the 24-h study (**b**). Impression: The findings are suggestive of an infected hematoma on the right side of the skull. The patient was taken to surgery immediately after the scan and approximately 300 mL of pus was drained from the scalp lesion

Case 11.5 Inflammatory Bowel Disease, Tc-WBC (Fig. 11.5)

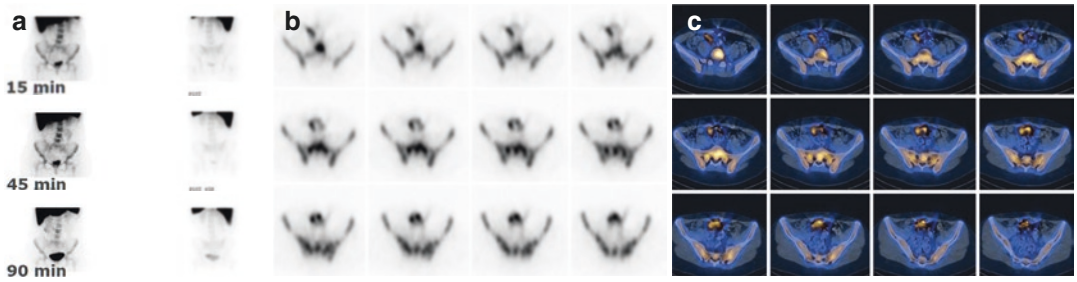

Fig. 11.5 History: An 18-year-old girl presenting with recurrent abdominal pain, fecal blood, and watery stool was evaluated with a Tc-WBC study for the clinical suspicion of inflammatory bowel disease. Study report: Planar scans at 15 and 45 min after tracer injection (**a**) show an area of abnormal tracer uptake in the right abdomen. Transaxial SPECT (**b**) and SPECT/CT (**c**) slices at the level of the lower abdomen localize this focus of uptake to the terminal ileum. A delayed planar scan (**a**, bottom row) performed at 90 min post-injection shows the progression of the tracer activity into the ascending colon. Impression: The findings suggest terminal ileitis, further confirmed at endoscopy

Case 11.6 Chronic Recurrent Multifocal Osteomyelitis, FDG (Fig. 11.6)

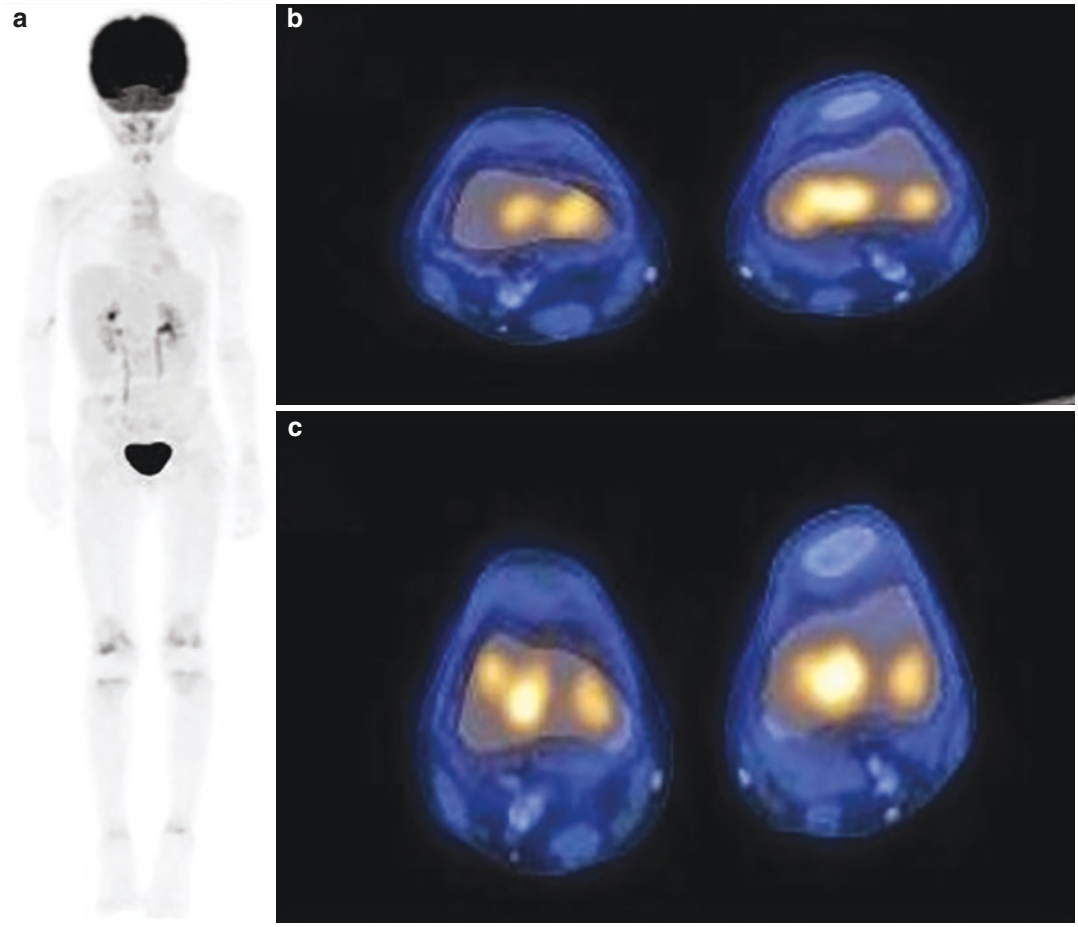

Fig. 11.6 History: A 7-year-old girl presented with joint pain, fever, and abnormal lab tests (elevated ESR, CRP, ASLO). Bone scintigraphy and abdominal US were normal and she was referred to PET/CT with FDG for further evaluation. Study report: Whole body maximum intensity projection (MIP) of the PET component (**a**) shows focally increased tracer uptake in both knees, involving the femoral and tibial metaphyses, also seen on transaxial PET/CT slices (**b**, **c**), as well as in both ankles, with no corresponding CT abnormalities. Impression: The findings suggest multifocal osteomyelitis, but a different etiology involving the bony structures cannot be excluded. Further evaluation with MRI was suggested. MRI of the left knee (not shown) demonstrated bone marrow edema, mild periostitis, and joint effusion. The differential diagnosis included chronic recurrent multifocal osteomyelitis, leukemia infiltration, and eosinophilic granuloma. Tissue sampling was recommended. CT-guided biopsy of the left distal femur demonstrated the presence of marked fibrosis, reactive trabecular changes, and focal neutrophil infiltration, with no evidence of leukemic infiltrates. The patient was diagnosed with chronic recurrent osteomyelitis and subsequently showed a good response to treatment with methotrexate and steroids

Case 11.7 Fever of Unknown Origin (FUO), Aspergillosis, FDG (Fig. 11.7)

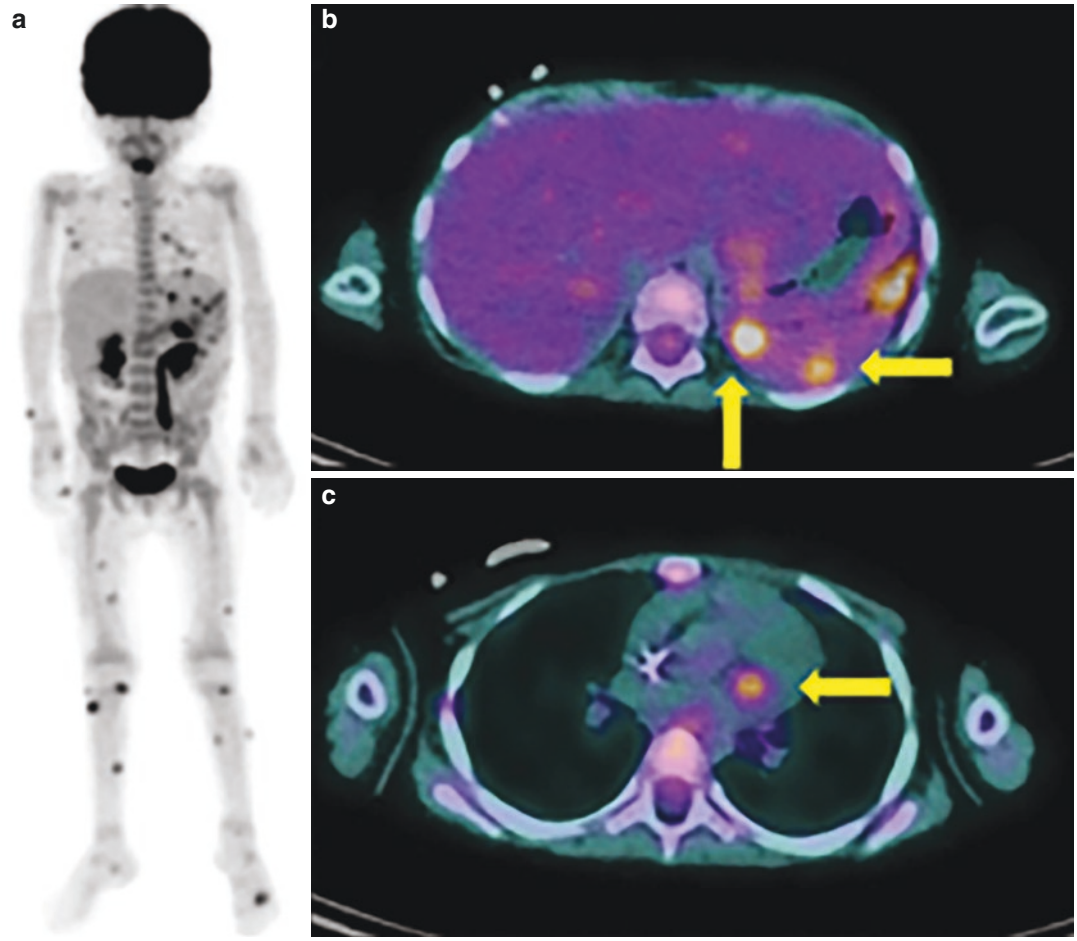

Fig. 11.7 History: A 2-year-old girl with leukemia developed pancreatitis secondary to chemotherapy followed by a persistent fever that did not respond to antibiotics. CT showed mild inflammatory changes in the lungs. A whole-body FDG PET/CT was performed to look for occult infective or inflammatory sites. Study report: FDG PET MIP image (**a**) and selected axial PET/CT slices at the level of the upper abdomen and chest (**b**, **c**) show multiple foci of abnormal tracer uptake throughout the subcutaneous and soft tissues, the lungs, pancreas, and spleen (yellow arrows), with a specific focal site of uptake in the heart (**c**, yellow arrow). Impression: The findings are suggestive of possible mycotic deposits. Biopsy and culture of a skin lesion revealed *Aspergillus*. Following a change of treatment to more specific antifungal agents, the patient's clinical status improved. On a repeat PET/CT study performed 2 months later (not shown), there is marked improvement with the disappearance of most tracer avid foci

Case 11.8 FUO, Septic Emboli, FDG (Fig. 11.8)

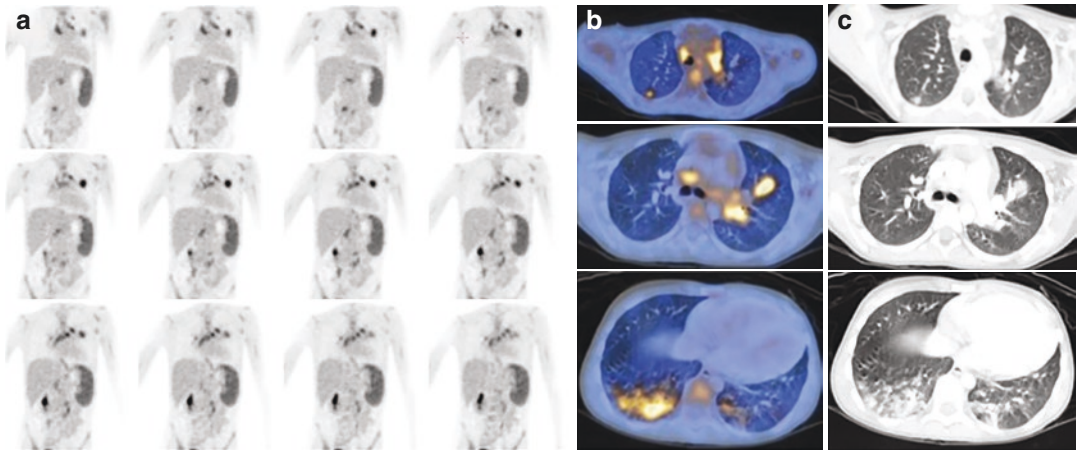

Fig. 11.8 History: A 7-year-old girl presented with fever, 39 °C, for 3 weeks. She had been previously diagnosed and treated for a urinary tract infection. She had positive blood cultures and echocardiography demonstrated the presence of endocarditis. FDG PET/CT was performed for further evaluation of potential extracardiac foci of infection. Study report: Coronal PET slices (**a**) show foci of increased tracer uptake in both lungs. Selected transaxial PET/CT (**b**) and CT (**c**) of the chest localize these sites of increased uptake to nodules and ground-glass opacities in both upper lung lobes and in a right lower lobe consolidation. Note also increased FDG uptake in an enlarged spleen. Impression: The findings are consistent with septic pulmonary emboli. Hypermetabolic splenomegaly is considered to be reactive to the infectious process

Case 11.9 FUO, Pericarditis, FDG (Fig. 11.9)

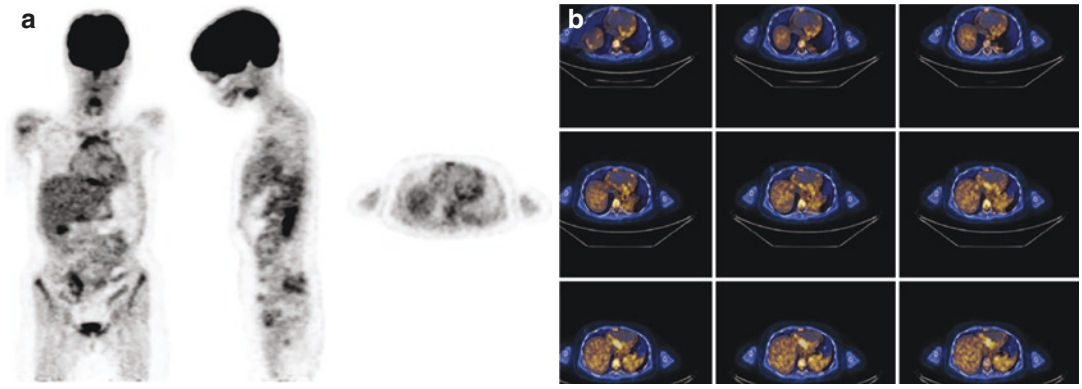

Fig. 11.9 History: An 8-year-old girl previously treated for pneumonia complained of fever (39.4 C) for three weeks. C-reactive protein was elevated. Abdominal US was normal. A whole-body FDG PET/CT was performed in search of a focal etiology that could explain the high, prolonged fever. Study report: Selected coronal, sagittal, and transaxial PET slices (**a**) show increased linear tracer uptake located in thickened pericardium and mild pericardial effusion surrounding the heart as demonstrated on transaxial PET/CT slices of the thorax (**b**). In addition, note physiologic tracer uptake in the thymus. Impression: The findings suggest the presence of pericarditis. Cardiac echography showed a new pericardial effusion. The patient was diagnosed with acute pericarditis and idiopathic juvenile arthritis and showed an excellent response to treatment with NSAIDS

Case 11.10 Vasculitis, FDG—PET/MRI (Fig. 11.10)

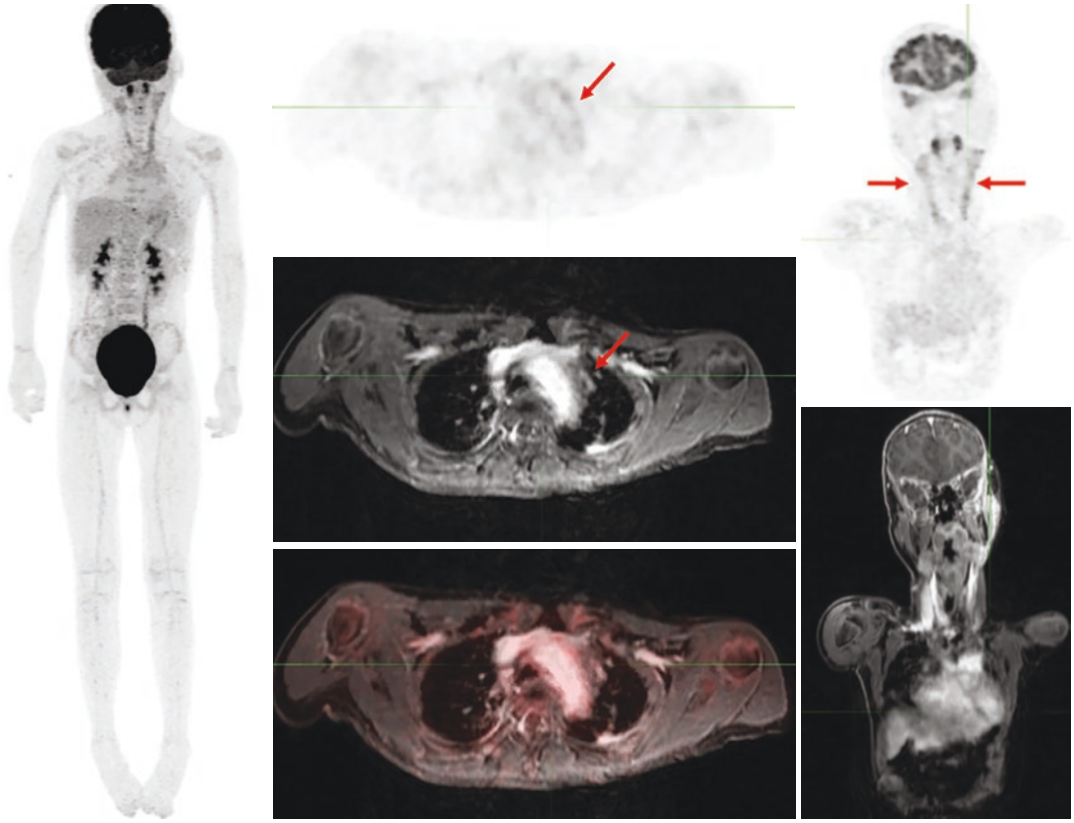

Fig. 11.10 History: A 12-year-old girl presented with persistent thoracic level back pain, intermittent fever, and elevated ESR. Cross-sectional imaging showed thickening of her aortic arch and bilateral great vessels. Takayasu's arteritis was diagnosed, and the patient was referred to FDG PET/MRI. Study report: The PET/MRI study (left PET-MIP, center column selected transaxial thoracic PET, MRI, and PET/MRI slices, right selected coronal cervical PET and MRI slices) shows increased FDG uptake in wall thickening of the left common carotid artery, extending from the origin to the bifurcation, and, to a lesser extent, along the caudal aspect of the right common carotid artery near the origin (arrows). In the chest, there is increased uptake in mild wall thickening of the thoracic aorta, involving the ascending and descending parts and the aortic arch (arrows). There is also mildly increased radiotracer uptake in the walls of the abdominal aorta, extending to the proximal iliac arteries. There is no abnormal metabolic activity or wall thickening involving the abdominal great branching arteries including the celiac axis, and the superior mesenteric and inferior mesenteric arteries. Impression: Multifocal mild wall thickening and increased metabolic activity of the left more than right common carotid arteries, thoracic and abdominal aorta, and proximal common iliac arteries. The increased metabolic activity suggests the presence of active arteritis

References

1. Signore A, et al. Nuclear medicine imaging in pediatric infection or chronic inflammatory diseases. Semin Nucl Med. 2017;47(3):286–303.
2. Parisi MT, et al. Radionuclide imaging of infection and inflammation in children: a review. Semin Nucl Med. 2018;48(2):148–65.
3. Ropers FG, et al. Evaluation of FDG-PET/CT use in children with suspected infection or inflammation. Diagnostics (Basel). 2020;10(9):715.
4. Sturm E, et al. Fluordeoxyglucose positron emission tomography contributes to management of pediatric liver transplantation candidates with fever of unknown origin. Liver Transpl. 2006;12(11):1698–704.
5. Wang SS, et al. The clinical utility of fluorodeoxyglucose-positron emission tomography

for investigation of fever in immunocompromised children. J Paediatr Child Health. 2018;54(5):487–92.
6. Pijl JP, et al. Role of FDG-PET/CT in children with fever of unknown origin. Eur J Nucl Med Mol Imaging. 2020;47(6):1596–604.
7. Chang L, et al. Search of unknown fever focus using PET in critically ill children with complicated underlying diseases. Pediatr Crit Care Med. 2016;17(2):e58–65.
8. Signore A, et al. Clinical indications, image acquisition and data interpretation for white blood cells and anti-granulocyte monoclonal antibody scintigraphy: an EANM procedural guideline. Eur J Nucl Med Mol Imaging. 2018;45(10):1816–31.
9. Charron M. Pediatric inflammatory bowel disease imaged with Tc-99m white blood cells. Clin Nucl Med. 2000;25(9):708–15.
10. Drubach LA. Nuclear medicine techniques in pediatric bone imaging. Semin Nucl Med. 2017;47(3):190–203.
11. Van den Wyngaert T, et al. The EANM practice guidelines for bone scintigraphy. Eur J Nucl Med Mol Imaging. 2016;43(9):1723–38.
12. Palestro CJ. Infection and inflammation. In: Treves ST, editor. Pediatric nuclear medicine and molecular imaging. New York: Springer; 2014. p. 541–69.
13. Aydın F, Kın Cengiz A, Güngör F. Tc-99m labeled HMPAO white blood cell scintigraphy in pediatric patients. Mol Imaging Radionucl Ther. 2012;21(1):13–8.
14. de Vries EF, et al. Guidelines for the labelling of leucocytes with (99m)Tc-HMPAO. Inflammation/Infection Task group of the European Association of Nuclear Medicine. Eur J Nucl Med Mol Imaging. 2010;37(4):842–8.
15. Servaes S. Imaging infection and inflammation in children with (18)F-FDG PET and (18)F-FDG PET/CT. J Nucl Med Technol. 2011;39(3):179–82.
16. Houseni M, et al. Applications of PET/CT in pediatric patients with fever of Unknown Origin. PET Clin. 2008;3(4):605–19.
17. Vali R, et al. SNMMI Procedure Standard/EANM Practice Guideline on Pediatric (18)F-FDG PET/CT for Oncology 1.0. J Nucl Med. 2021;62(1):99–110.
18. Dhar AV, et al. Team Approach: Pediatric Musculoskeletal Infection. JBJS Rev. 2020;8(3):e0121.
19. Rabkin Z, Israel O, Keidar Z. Do hyperglycemia and diabetes affect the incidence of false-negative 18F-FDG PET/CT studies in patients evaluated for infection or inflammation and cancer? A Comparative analysis. J Nucl Med. 2010;51(7):1015–20.
20. Kagna O, et al. Does Antibiotic Treatment Affect the Diagnostic Accuracy of (18)F-FDG PET/CT Studies in Patients with Suspected Infectious Processes? J Nucl Med. 2017;58(11):1827–30.
21. Bagrosky BM, et al. 18F-FDG PET/CT evaluation of children and young adults with suspected spinal fusion hardware infection. Pediatr Radiol. 2013;43(8):991–1000.
22. Warmann SW, et al. Follow-up of acute osteomyelitis in children: the possible role of PET/CT in selected cases. J Pediatr Surg. 2011;46(8):1550–6.
23. Jasper N, et al. Diagnostic value of [(18)F]-FDG PET/CT in children with fever of unknown origin or unexplained signs of inflammation. Eur J Nucl Med Mol Imaging. 2010;37(1):136–45.
24. del Rosal T, et al. ^{18}F-FDG PET/CT in the diagnosis of occult bacterial infections in children. Eur J Pediatr. 2013;172(8):1111–5.